Numerical Calculation for Asynchronous Magnetic Coupling

Kaikai Zhou[1], Peng Wang[1], Zhi Yuan [1]and Yanjun Ge[1]
[1]*College of Mechanical Engineering, Dalian Jiaotong University, Huanghe Street, Shahekou Distict, China*

Keywords: Asynchronous magnetic coupling, Mechanical properties, Magnetic field analysis, Vector magnetic potential

Abstract: The available magnetic circuit algorithm is difficult to calculate exactly the electromagnetic torque of the asynchronous magnetic coupling (AMC). The present study establishes the gap flux density theory model by the use of vector magnetic potential method and the two-dimensional field boundary condition, and then analyzes the variation law of induction current among the cage bars along with the spatial phase and electric angle. The Lorenz force is integrated around the circumferential direction, and then the electromagnetic torque model was established according to the current superposition principle. The obtained theoretical gap flux density, cage bars induced current and torque were analyzed comparatively with the finite element method. The revolving speed curve, torque curve and current curve of AMC under rated condition were obtained by the method of finite element dynamic analysis, and then the electromagnetic torque characteristic curve was draw to reveal its dynamic operation law. At last, the correctness of the mechanical characteristics of AMC was verified by experimental results.

1 INTRODUCTION

In recent years, adjustable-speed magnetic couplings have been very successfully introduced to provide a high-efficiency alternative means of control by matching the motor output speed and torque to the requirements of the load[1, 2]. Compared with the ordinary couplings, magnetic coupling has the advantages of non-contact power transmission, no friction, stable transmission, low working condition, low maintenance cost, etc. Compared with variable-frequency drives (VFD)[3], magnetic coupling do not generated electronic harmonics which will cause system problems and may overheat motor windings.

The squirrel cage rotor has been tested for a long time, and the theory is relatively mature. Therefore, the use of standard squirrel cage rotor design magnetic coupling has the advantages of low design cost, easy to manufacture, and can be applied to the field of electromagnetic braking, and has attracted widespread attention of scholars. The Flux Drive company in the United States has commercial production of speed adjustable squirrel cage rotor couplings, but its cage rotor needs to be redesigned and has a longer design cycle, and there is no literature to report its mechanical properties[4]. To solve this problem, an asynchronous magnetic coupling based on an existing squirrel cage rotor is proposed[5,6].

The mechanical analysis of magnetic drive mainly includes analytic method[7,8] and finite element method[9,10]. In this paper, the two methods are combined to do the following research work: the gap flux density theory model is established by the use of vector magnetic potential method, and then the variation law of induction current among the cage bars along with the spatial phase and electric angle are analyzed. The torque is analyzed by Faraday law of electromagnetic induction. The obtained theoretical gap flux density, cage bars induced current and torque are analyzed comparatively with the finite element method.

2 STRUCTURE OF AMC

The asynchronous magnetic coupling is mainly composed of the outer rotor, the squirrel cage rotor and the air gap. The structure of the asynchronous magnetic coupling is shown in Fig.1.

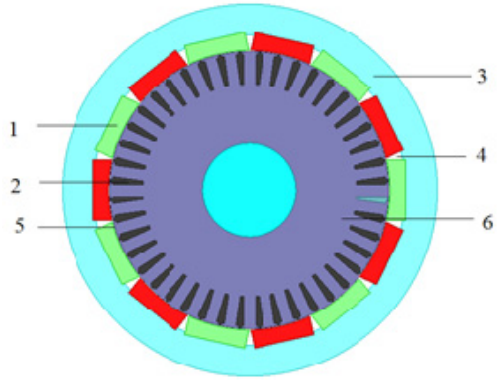

1. Permanent magnet 2. Cage bar 3. Yoke 4. Fill block（Non-magnetic material） 5. Air gap 6. Cage rotor

Figure 1: The structure of the asynchronous magnetic coupling.

3 TORQUE CALCULATION

The air gap magnetic field plays a decisive role in the torque transmission of the asynchronous magnetic coupling. Paper [1] has calculated the radial component B_r and the tangential component B_θ of the air gap magnetic field by using the vector magnetic potential method. The formula is as follows:

$$B_{1r}(r,\theta)=\sum_{n=1}^{\infty} np\left(A_{n1}r^{np-1}+B_{n1}r^{-np-1}\right)\cos(np\theta) \quad (1)$$

$$B_{1\theta}(r,\theta)=-\sum_{n=1}^{\infty} np\left(A_{n1}r^{np-1}-B_{n1}r^{-np-1}\right)\sin(np\theta) \quad (2)$$

Where p is the pole-pairs of permanent magnet, r is the air gap radius, A_{n1} and B_{n1} are constants for calculation, the formula is as follows:

$$A_{n1}=\frac{\mu_0 M_n R_1^{-2np}\begin{bmatrix}\left(R_2^{-2np}+R_3^{-2np}\right)\left(R_3^{np-1}-R_2^{np-1}\right)\\+\left(npR_3^{np-1}-R_2^{np-1}\right)\left(R_2^{-2np}-R_3^{-2np}\right)\end{bmatrix}}{R_2^{np-1}R_3^{np-1}\begin{bmatrix}\mu_r\left(R_1^{-2np}-R_2^{-2np}\right)\left(R_2^{-2np}+R_3^{-2np}\right)\\+\left(R_2^{-2np}-R_3^{-2np}\right)\left(R_1^{-2np}+R_2^{-2np}\right)\end{bmatrix}\left[(np)^2-1\right]} \quad (3)$$

$$B_{n1}=\frac{\mu_0 M_n\begin{bmatrix}\left(R_2^{-2np}+R_3^{-2np}\right)\left(R_3^{np-1}-R_2^{np-1}\right)\\+\left(npR_3^{np-1}-R_2^{np-1}\right)\left(R_2^{-2np}-R_3^{-2np}\right)\end{bmatrix}}{R_2^{np-1}R_3^{np-1}\begin{bmatrix}\mu_r\left(R_1^{-2np}-R_2^{-2np}\right)\left(R_2^{-2np}+R_3^{-2np}\right)\\+\left(R_2^{-2np}-R_3^{-2np}\right)\left(R_1^{-2np}+R_2^{-2np}\right)\end{bmatrix}\left[(np)^2-1\right]} \quad (4)$$

Where μ_0 is the vacuum permeability, and the M_n is the coefficients of the Fourier series expansions (n=1, 2...), R_1 is the outer diameter of the squirrel cage rotor, R_2 is the inner diameter of the permanent magnet, and R_3 is the outer diameter of the permanent magnet.

The induction electromotive force in each cage bar of the squirrel cage rotor is proportional to the magnetic field density, and the current direction can be determined by the right-hand rule.

According to Faraday's electromagnetic induction theorem, the maximum induction potential induced by cutting magnetic induction lines in each cage is as follows:

$$E_{s\max}=B_r L v \quad (5)$$

Where v is the relative rotation speed of internal and external rotor, and

$$v=\frac{\pi D(n_z-n_l)}{60}=2\frac{\pi D}{2p}\cdot\frac{p(n_z-n_l)}{60}=2\tau f \quad (6)$$

Because the squirrel cage rotor winding is self-closing and the loop is formed, the terminal voltage is in short-circuit state, and its terminal voltage is zero. Each loop is routed by two cage bars, so that the total potential in the circuit $E_N=2E_S$. According to Kirchhoff's second law, the voltage balance equation in the rotor winding is as follows:

$$2\dot{E}_s-\dot{I}Z_{\sigma s}=0 \quad (7)$$

$$\dot{I}=\frac{2\dot{E}_s}{Z_{\sigma s}}=\frac{2s\dot{E}}{R_B+jsX_\sigma} \quad (8)$$

The effective value of the rated current is as following:

$$I=\frac{2sE}{\sqrt{R_B^2+(sX_\sigma)^2}} \quad (9)$$

The expression for the electromagnetic torque can be expressed as follows:

$$T = \sum_{i=1}^{Z_0} T_0 = 4sZ_0 B_\delta^2 L^2 \frac{\pi f_z w k_w}{p\sqrt{R_B^2 + (sX_\sigma)^2}} = sZ_0 B_\delta^2 L^2 \frac{\pi n_z w k_w}{15\sqrt{R_B^2 + (sX_\sigma)^2}} \quad (10)$$

4 FINITE ELEMENT ANALYSIS

The model parameters are shown in Table 1.

2-Dimension model is established according to Tab.1 model parameters. Defining material attribute: the materials of air gap, outer rotor, inner rotor and permanent magnets should be defined when analyzing the asynchronous magnetic coupling. The model is divided into meshes, the result is shown in Fig.2.

Table 1: Model parameters of SCRMC.

Name	numerical value
Pole pair of permanent magnet	7
The outer diameter of the yoke /mm	120
The outer diameter of the permanent magnet /mm	100
The inner diameter of the permanent magnet /mm	90
The outer diameter of squirrel-cage rotor /mm	89.35
The inner diameter of squirrel-cage rotor /mm	30
Air gap /mm	0.65
Axial length /mm	85

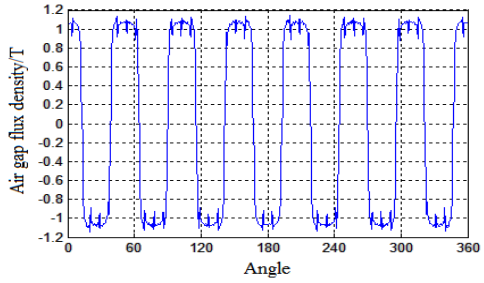

Figure 2: Radial air gap flux density diagram.

The remanence of the permanent magnet material is 1.18T. In Fig.1, the average value of the air gap magnetic density is about 1.1T, and the air gap magnetic density distribution fluctuates slightly. The minimum value is 0.9T, and the maximum value is 1.18T, which indicates that there is leakage.

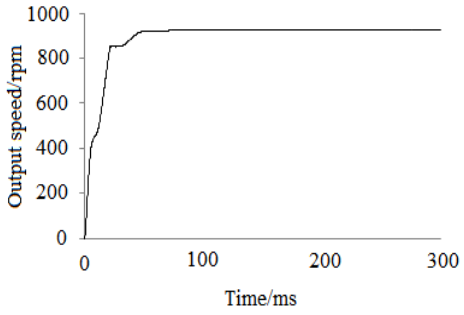

Figure 3: Speed diagram for AMC.

Using the dynamic analysis model, adding motion conditions of outer rotor and an inner rotor, and the setting conditions are as follows: outer rotor speed is set to 1000 rpm, the initial rotational speed of the inner rotor is set to 0 rpm, the moment of inertia is 0.094 kgm2, the output power is 30 kW, the solution time is 0.3 s, the step is set to 0.0004 s. After the solution and the post-processing, the results are obtained respectively, as shown in Fig.3 and Fig.4.

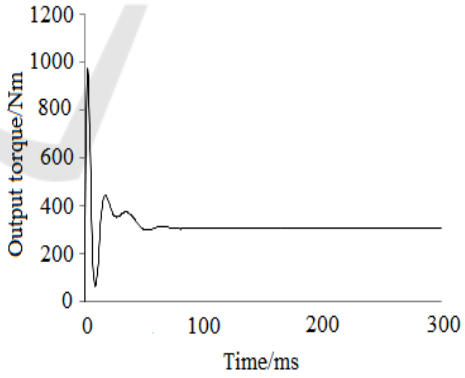

Figure 4: Torque diagram for AMC.

In order to further study the mechanical characteristics of AMC, external rotor speed is fixed as 1000 rpm and only the squirrel cage rotor speed is changed, the cage rotor inertia, damping and other mechanical properties are not considered. The final mechanical characteristics of AMC are shown in Fig.5.

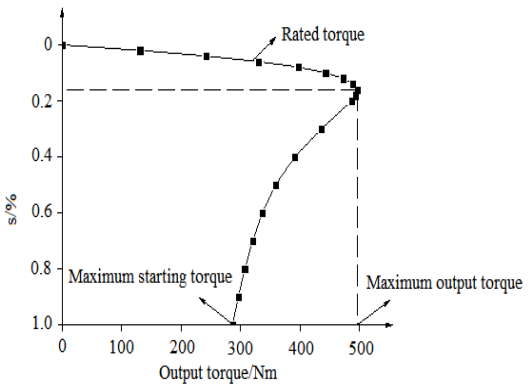

Figure5: Mechanical characteristic diagram.

As shown in Figure 5: the mechanical properties of AMC and three-phase asynchronous motor are similar, slip ratio and torque are on a linear relationship above the maximum torque, and on a nonlinear relationship between the maximum torque and maximum starting torque; the maximum torque0 Tm is 502.9 Nm, the corresponding slip is 0.18. The maximum torque is greater than the rated torque, which means that the AMC has overload ability. The maximum starting torque is 306.8 Nm, and the load torque from the start to the steady-state is less than the corresponding torque from the motor mechanical characteristic curve, which in accordance with the design requirements of the working conditions.

5 CONCLUSIONS

In this paper, the static air gap magnetic field is analyzed by ANSYS software, in good agreement with the analytical method. The mechanical performance of the squirrel cage rotor magnetic coupling is analyzed from the start to the steady state when the actual load is simulated by dynamic analysis. When running stably, the output torque is 923.5 rpm and the output torque is 385.3 Nm; its mechanical characteristic curve is also given.

ACKNOWLEDGEMENTS

This work is supported by Project of National Natural Science Foundation of China (No. 51285092), all support is gratefully acknowledged.

REFERENCES

1. Fujun H E, Zhong Y, Zhang R, et al. Research on Characteristics of Permanent Magnet Eddy-current Coupling Drive[J]. Journal of Mechanical Engineering, 2016.
2. Li K, Bird J Z, Acharya V M. Ideal Radial Permanent Magnet Coupling Torque Density Analysis[J]. IEEE Transactions on Magnetics, 2017, PP(99):1-1.
3. Cuzner R, Drews D, Kranz W, et al. Power-Dense Shipboard-Compatible Low-Horsepower Variable-Frequency Drives[J]. IEEE Transactions on Industry Applications, 2013, 48(6):2121-2128.
4. http://www.fluxdrive.com
5. Yanjun G E, Zhang S, Jiang Y, et al. Analysis and calculation of the torque characteristics of squirrel cage asynchronous magnetic coupling[J]. Modern Machinery, 2015.
6. Zhou K, Yuan Z, Wang P, et al. Numerical calculation for axial force of Adjustable Speed Asynchronous Magnetic Coupling[C]// Progress in Electromagnetic Research Symposium. 2016:1487-1491.
7. Y. J. Ge，C. Y. Nie，Q. Xin．A three dimensional analytical of the air-gap magnetic field and torque of coaxial magnetic gears．Progress In Electromagnetics Research，2012, 131:391-407.
8. Anglada J R, Sharkh S M. Analytical calculation of air-gap magnetic field distribution in transverse-flux machines[C]// IEEE International Symposium on Industrial Electronics. IEEE, 2016.
9. Yang C J, Li Q W, Ma H L, et al. Numerical Analysis of Electromagnetic Field of Solid Rotor Asynchronous Permanent Magnetic Coupling by Finite Element Method[C]// Materials Science Forum. 2008:1376-1381.
10. Yang C J, Yan-Fei X U, Kong L Y, et al. Finite element analysis of Halbach array circuit of field-modulated asynchronous magnetic coupling[J]. Journal of Magnetic Materials & Devices, 2014.